https://doi.org/10.30799/jnst.311.20060305 J. Nanosci. Tech. - Volume 6 Issue 3 (2020) 915–917

ISSN: 2455-0191

Share Your Innovations through JACS Directory

Journal of Nanoscience and Technology

Visit Journal at https://www.jacsdirectory.com/jnst

Synthesis of Metal Doped TiO_2 Nano-Composites by Sol-Gel Method and Their Structural Properties

Altaf Rajani, Jyoti Sharma, Pranav Y. Dave*

Institute of Research and Development, Gujarat Forensic Sciences University, Gandhinagar – 382 007, Gujarat, India.

ARTICLEDETAILS

Article history:
Received 13 September 2020
Accepted 21 September 2020
Available online 28 September 2020

Keywords:
Nano-Composites
Zn Doped TiO_2
Zr Doped TiO_2

ABSTRACT

Metal oxide nano-composites plays a very important role in many areas of chemistry, physics and material science. This paper explains the synthesis and comparison of zinc and zirconium doped TiO_2 metal oxide nano-composites and their different properties. Here the sol-gel method is used to synthesis both the nano-composites. Nano-composites have been characterized with XRD, AFM, Zetasizer & potential and FT-IR studies. XRD study revealed good crystallinity with the size range of 30 nm – 45 nm for both nano-composites. AFM studies also revealed the same. FTIR study reports the characteristics peaks of synthesised nano-composites.

1. Introduction

Nowadays, nano-composites are widely used in research areas and provide benefits in future also: Drug delivery system, anti-corrosion barrier coating, lubricants and scratch free paints, new fire-retardant materials, new scratch/abrasion resistant materials, Superior strength fibers and films [1]. Different types of nano-composites are mainly used in industrial areas like MgO_2 and other alkaline earth oxides are widely used in chemical industry as a scrubber for air pollutant gases and as a catalyst support. ZrO_2 can be used as a structural ceramic, solid electrolyte, gas sensor and as a catalyst. Varieties of nano-composites have depending upon the types of matrix used and they are classified into three different categories as polymer matrix nano-composites, ceramic matrix nano-composites and metal matrix nano-composites [2, 3]. Metal oxide nano-composites are used in various important areas like detection of pesticides and toxins in food beverages, detection of organic and inorganic pollutants in water, drug detection [4, 5]. They are also used most effectively in the discipline of forensic toxicology for examination of different toxic materials from numerous important forensic evidences like hair, blood, saliva, vitreous humor and even from remains of body skeleton and samples of evidences of fingerprint. And also used to detection of heavy chemicals in organic foods. Nano-composites are also used for biomedical application such as tissue engineering, drug delivery, cellular therapies. Because of unique interactions between polymer and nano-particles, a range of property combinations can be engineered to mimic native tissue structure and properties [6,7].

The use of different nano-composite as a photocatalyst has been extensively studied in order to decompose various kinds of organic pollutants because of their high oxidative power, non-toxicity, photostability, and water insoluble properties under most conditions.

Pure Zn and Cr doped TiO_2 nanoparticles had been synthesized using combustion method by Pawar et al. [8]. The photocatalytic activities of the catalysts were tested under UV light for the degradation of phenol as a probe molecule. XRD results confirmed that Zn doping significantly inhibit the anatase-to rutile phase transformation and rutilation was promoted with Cr doping. Nguyen et al. [9] synthesised Zn-doped anatase TiO_2 nanoparticles by single step hydrothermal method. They found that incorporation of Zn^{2+} into an anatase lattice elevates the edge of the conduction band (CB) of the photoanodes and the Fermi level is shifted toward the CB edge, which contributes to the improvement in open-circuit voltage (V_{OC}). Chang et al. studied catalytic activity of Zr and Ag co-doped TiO_2 nanoparticles on the reduction of 4-nitrophenol, degradation of methylene blue and methyl orange was studied using sodium borohydride as reducing agent [10].

This present study made an attempt to synthesis Zn doped TiO_2 nanocomposite and Zr doped TiO_2 nanocomposite using sol-gel route.

2. Experimental Methods

2.1 Materials and Instruments

All the materials and solvents were purchased from commercial sources (Sisco research laboratories Pvt. Ltd., India, Sigma Aldrich and Abhishek Enterprise) and used as received unless stated otherwise. Ethanol (extra pure AR, 99.9%), acetic acid (extra pure AR, 99.5%), zinc chloride (anhydrous, 97%), titanium isopropoxide (AR, 97%), isopropanol (HPLC grade, 99.8%), zirconyl nitrate (anhydrous, 99.5%) and hydrazine hydrate (reagent grade, 99.8%) were obtained from SRL company and used without further purification process. Milli-Q water and spectroscopic grade solvents were used for all measurements. Fourier-transform infrared (FTIR) spectra were measured using JASCO FT-4600 spectrophotometer by putting directly the powder sample into it. For the analysis of structural property, GNR APD 2000 P-XRD instrument was used at room temperature without removing dissolved O_2. Atomic force microscopy (Nanosurf C300) was used to find the particle size after diluting the powder sample into ethanol and dried it on MICA sheet at room temperature.

2.2 Synthesis of Zn Doped TiO_2

The synthesis was done by the procedure explained by Shuo Pang et al. [11]. In brief, sol-gel method was used to synthesis Zn doped TiO_2 nanocomposites. In a single neck round bottom flask, 2.6 mL of zinc chloride solution (33 mg in 5 mL Milli-Q water), 4 mL of acetic acid, 3 mL of Milli-Q water and 12 mL of ethanol were taken. The solution was mixed using stirrer for better mixing the solutes and solvents to each other. Then another solution of titanium isopropoxide (16 mL) and ethanol (40 mL) was prepared. Then this solution was drop wise added into the first solution slowly and stirred overnight. The gel occurred at the end of the process. The gel was kept in muffle furnace for 12 hours at 120 °C and followed by the wash with Milli-Q water. For calcinations process, the powder was calcined using muffle furnace for 1 hour at 180 - 200 °C.

*Corresponding Author:pranavdave77@yahoo.com(Pranav Y. Dave)

https://doi.org/10.30799/jnst.311.20060305

2.3 Synthesis of Zr Doped TiO_2

The synthesis was carried out by the previously published process of nanocomposite, which was done by Saraschand Narnginti et al. [12]. 3.5 mL of titanium isopropoxide was mixed with 25 mL HPLC grade isopropanol and left it for 15 minutes for stirring. Then Milli-Q water (100 mL) was added drop wise into the solution to reach pH 1.5. Then another solution was prepared by mixing zirconyl nitrate (850 mg) in Milli-Q water (2 mL). After stirring for an hour, the solution was added to the main solution. Now 3 mL of hydrazine hydrate was added into the solution, hence the solution colour was changed from transparent to yellow with some precipitation. For better result of the particles, the solution was kept into sonication for 90 minutes and followed by the calcination in a muffle furnace for 2 hours at 450 °C.

3. Results and Discussion

The structural properties of zinc oxide doped titanium dioxide and zirconium doped titanium dioxide were characterized by X-ray diffractometer (XRD) using GNR APD 2000, advance diffractometer with Cu-Kα radiation having wavelength 1.54 Å. Fig. 1 shows the XRD pattern of Zn doped TiO_2 and Zr doped TiO_2 nanocomposites. The XRD pattern of Zn doped TiO_2 shows different diffraction peaks which concludes the presence of (101), (004), (200) and (105) planes.

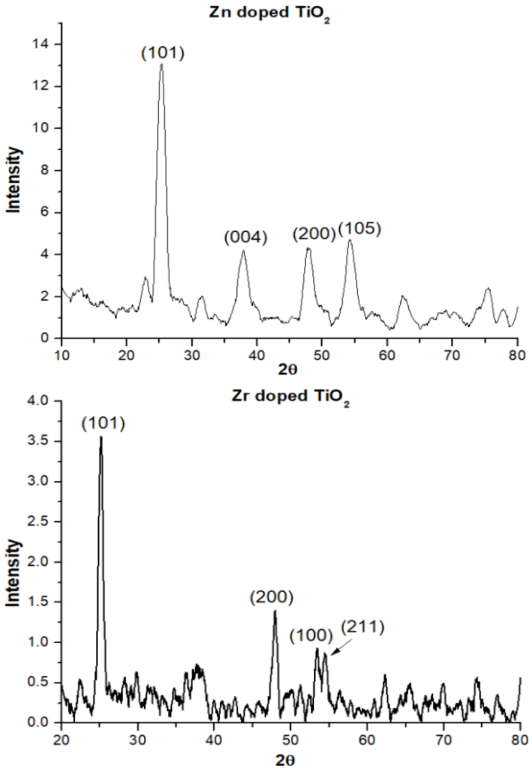

Fig. 1 XRD pattern of Zn doped TiO_2 and Zr doped TiO_2 nanocomposites

Here, the single diffraction peak (200) shows the presence of zinc in nanocomposite (JCPDS card no. 043-0002). This diffraction peak explained the wurtzite structure of zinc material. Other diffraction peaks (101) and (004) show the rutile structure of the TiO_2 (JCPDS card no. 21-1276). The content of zinc material in nanocomposite is very less with respect to the low intense diffraction peak of (200). But the content of TiO_2 is more with respect to high intense peak of (101). Similarly, XRD pattern of Zr doped TiO_2 reveals the content of TiO_2 is more with respect to the high and intense diffraction peak of (101); but the diffraction peak (100) shows the anatase structure of TiO_2 (JCPDS card no. 21-1272). As explained earlier, here the diffraction peak (200) shows the hexagonal structure of the zirconium. Both nanocomposites have TiO_2 which was confirmed from (101) diffraction peaks.

Debye Scherrer formula [13] was used to calculate the average crystallite size (*d)* of the samples as shown in Eq.(1):

$$d = \frac{0.9\lambda}{\beta cos\theta_B} \qquad (1)$$

where λ, θ_B and β are the X-ray wavelength (1.54056 Å), Bragg diffraction angle and line width at half maximum of the peak, respectively. The average crystallite size of Zn doped TiO_2 and Zr doped TiO_2 are 30 nm – 40 nm and 35 nm – 45 nm respectively. The average crystallite size is depending on the content of the TiO_2.

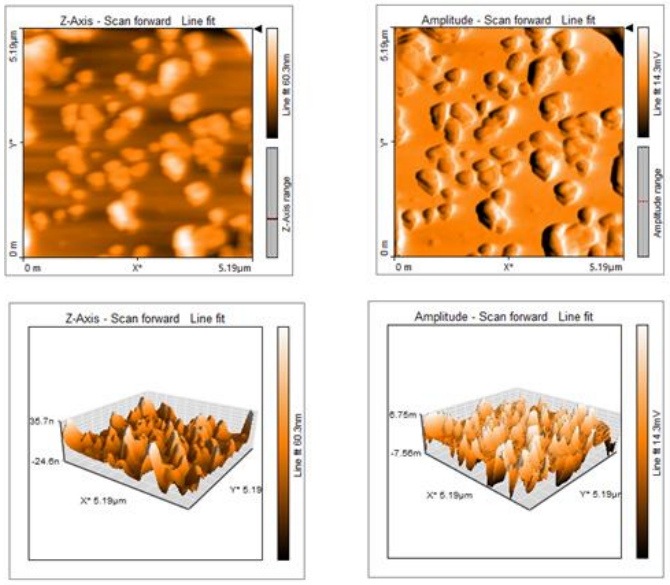

Fig. 2 AFM image of Zn doped TiO_2

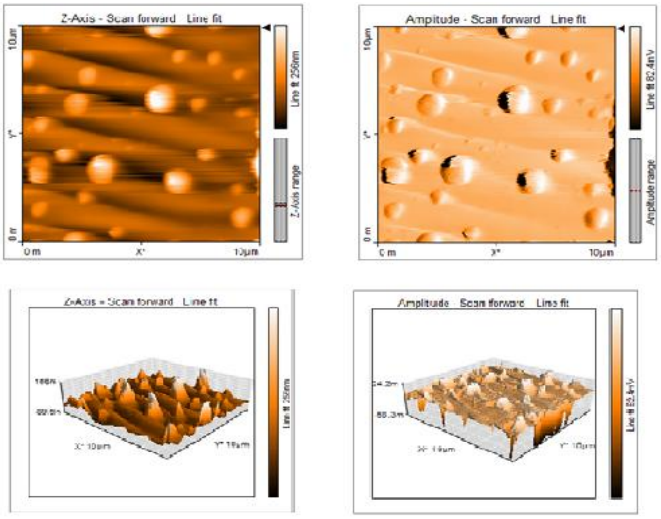

Fig. 3 AFM image of Zr doped TiO_2

Further the particle size was analysed by AFM instrument. Figs. 2 and 3 show the 2D and 3D pattern of Zn doped TiO_2 and Zr doped TiO_2 nanocomposites respectively. The images show the particle size of Zn doped TiO_2 and Zr doped TiO_2 are 34.9 nm and 47 nm respectively. The particle size was calculated by the Nanosurf C3000 model software. The software can be detected by the height of the particle, which was placed and dried at the top of the MICA plate. Rieth et al. [14] reported about the surface roughness that represents the standard deviation between the height of topographic features and the mean feature height. "Grain size" is determined by the stereological techniques. By using ethanol as a solvent to dry the powder sample on the MICA sheet, some nanoparticles became nanocluster to bind with each other. But some nanocomposites are clearly appearing in AFM image.

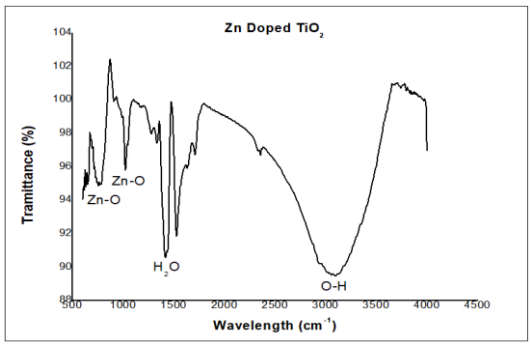

Fig. 4 FTIR spectra of Zn doped TiO_2

https://doi.org/10.30799/jnst.311.20060305

Further, to obtain structural property of nanocomposites, the FT-IR JASCO FT-4600 spectrophotometer was used. Fig. 4 shows FTIR spectra of Zn doped TiO_2. The absorption bands in range 500-1000 cm^{-1} represent Zn-O vibration. The absorption band around 3000 cm^{-1} shows stretching and bending O-H bond, which means there is presence of moisture. Fig. 5 shows the FTIR spectra of the Zr doped TiO_2. The absorption band in range 500-1000 cm^{-1} reveals the presence of Zr-O_2-Zr vibration bond. The absorption band present around 2500 cm^{-1} represents O-H bond, which is also representing some moisture inside the powder sample. Both the FTIR spectra represent peaks after 2500 cm^{-1} which shows the Ti-O bond and hence confirms the presence of TiO_2.

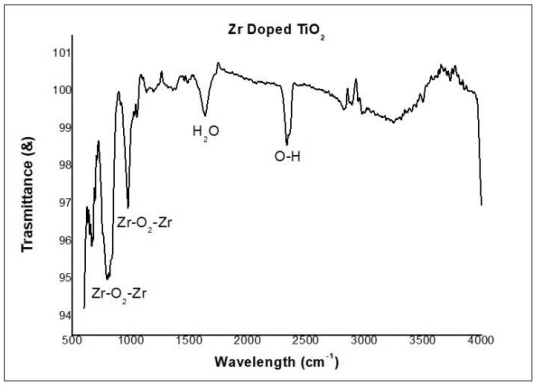

Fig. 5 FTIR spectra of Zr doped TiO_2

Figs. 6 and 7 show the particle distribution in the solution by Malvern Zetasizer DLS ZS instrument. It shows the average particle size, which would be dispersed in the solution.

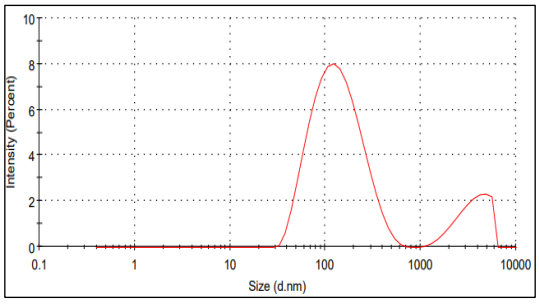

Fig. 6 Particle size distribution of Zn doped TiO_2 (DLS)

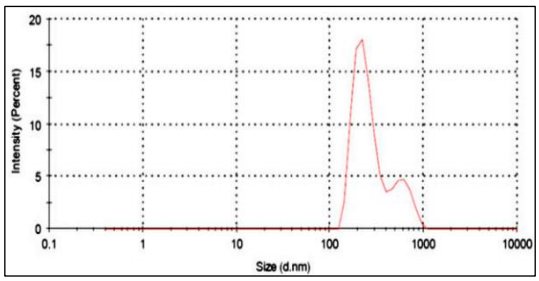

Fig. 7 Particle size distribution of Zr doped TiO_2 (DLS)

After dispersed the nanocomposite in ethanol, the instrument shows 134.7 d.nm of the average particle size. If the nanocomposite will disperse in Milli-Q water, then the average particle size was obtained as 150 d.nm. Fig. 7 shows the particle distribution of Zr doped TiO_2 nanocomposite. Here the particle distribution curve is little bit noisy with the solvent ethanol because of the vibration, which occurs in the cell. Dispersion is the effective parameter of the Zeta sizer DLS. The particles would be dispersed in proper way to get good and precise result about the particle size. In Zn doped TiO_2 nanocomposite graph, the particles are well dispersed in the solvent. So that the particle distribution curve is smooth and broad. But in Zr doped TiO_2 nanocomposite, the particles are big, so the curve is little bit sharp and bit noisy. Here the average particle is 145.8 d.nm.

4. Conclusion

As per the sol-gel route, the Zn doped TiO_2 nanocomposite and Zr doped TiO_2 nanocomposite were synthesised precisely. The nanocomposites are very crystalline as from the results of XRD. The sizes of the nanocomposites are obtained with the range of 30 nm - 45 nm. It was further confirmed by AFM studies. Also, FTIR study reveals the presence of synthesised composites. Therefore, the sol-gel method can be used to synthesis more metal based metal oxide nano-composites.

References

[1] Hongbo Gu, Chao Ma, Junwei Gu, Jiang Guo, Xingru Yan, Jiangnan Huang, Qiuyu Zhang, Zhanhu Guo, An overview of multifunctional epoxy nanocomposites, J. Mater. Chem. C 4 (2016) 5890–5906.
[2] J. Njuguna, K. Pielichowski, J. Fan, Polymer nanocomposites for aerospace applications, Woodhead Publishing Limited, Poland, 2012.
[3] Ping Xu, Xijiang Han, Bin Zhang, Yunchen Dua, Hsing-Lin Wang, Deep ultraviolet to near-infrared emission and photoresponse in layered n-doped graphene quantum dots, ACS Nano. 8 (2014) 6312–6320.
[4] A. Lateef, R. Nazir, Metal nanocomposites: Synthesis, characterization and their applications, Sci. Appl. Tailor. Nanostruct. 12 (2017) 239–256.
[5] N. Patelli, A .Migliori, V. Morandi, L. Pasquini, One-step synthesis of metal oxide nanocomposites by gas phase condensation, Nanomater. 9 (2019) 1–15.
[6] P.H.C. Camargo, K.G. Satyanarayana, F. Wypych, Nanocomposites: Synthesis, structure, properties and new application opportunities, Mater. Res. 12 (2009) 1–39.
[7] J. Li, S. Tang, L. Lu, H.C. Zeng, Preparation of nanocomposites of metals, metal oxides, and carbon nanotubes via self-assembly, J. Am. Chem. Soc. 129 (2007) 9401–9409.
[8] M.J. Pawar, V.B. Nimbalkar, Synthesis and phenol degradation activity of Zn and Cr doped TiO_2 Nanoparticles, Res. J. Chem. Sci. 2 (2012) 32–37.
[9] T.B. Nguyen, M.J. Hwang, K.S. Ryu,Synthesis and high photocatalytic activity of Zn-doped TiO_2, Bull. Korean Chem. Soc. 33 (2012) 1–5.
[10] S.M. Chang, R.A. Doong, Characterization of Zr-doped TiO_2 nanocrystals prepared by a nonhydrolytic sol-gel method at high temperatures, J. Phys. Chem. B 110 (2006) 20808–20814.
[11] Shuo Pang, Ji-guo Huang, Yun Su, Bo Geng, Su-yuan Lei, et al., Synthesis and modification of Zn-doped TiO_2 nanoparticles for the photocatalytic degradation of tetracycline, Photochem. Photobiol. 92 (2016) 651–657.
[12] S. Naraginti, F.B. Stephen, A. Radhakrishnan, A. Sivakumar, Zirconium and silver co-doped TiO_2 nanoparticles as visible light catalyst for reduction of 4-nitrophenol, degradation of methyl orange and methylene blue, Spectrochim. Acta A: Mol. Biomol. Spectrosc. 135 (2015) 814–819.
[13] A.M. Rosa, E.P.da. Silva, E. Amorim, M. Chaves, A.C. Catto, et al., Growth evolution of ZnO thin films deposited by RF magnetron sputtering, J. Phys. Conf. Ser. 370 (2012) 1-7.
[14] L.W. Rieth, Sputter deposition of ZnO films, University of Florida, USA, 2001.

https://doi.org/10.30799/jnst.311.20060305

Cite this Article as: Altaf Rajani, Jyoti Sharma, Pranav Y. Dave, Synthesis of metal doped TiO_2 nano-composites by sol-gel method and their structural properties, J. Nanosci. Tech. 6(3) (2020) 915–917.